

Identification of differentially expressed genes associated with ferroptosis in Crohn's disease

WENQUAN ZHANG^{1*}, ZHAOSHUI LI^{1*}, HONGBO LI² and DIANLIANG ZHANG²

¹Qingdao Medical College, Qingdao University, Qingdao, Shandong 266000; ²Department of The First General Surgery, Qingdao Hospital, University of Health and Rehabilitation Sciences (Qingdao Municipal Hospital), Qingdao, Shandong 266011, P.R. China

Received September 26, 2023; Accepted November 17, 2023

DOI: 10.3892/etm.2024.12378

Abstract. Ferroptosis-related genes may play a critical regulatory role in the pathogenesis of Crohn's disease (CD). The purpose of the present study was to identify genes expressed in CD that are associated with ferroptosis, and to provide guidance in the diagnosis and therapy of CD. CD mRNA expression data were initially gathered from the Gene Expression Omnibus (GEO) database. GSE75214 and GSE102133 datasets were selected as the major targets and were analyzed for differentially expressed genes (DEGs). Subsequently, R software was used to analyze the common genes among the DEGs between CD and ferroptosis-related genes. Gene Ontology enrichment analysis and Kyoto Encyclopedia of Genes and Genome pathway analysis were conducted to identify related pathways and functions. Protein-protein interaction (PPI) analysis was performed to identify target genes. The DSigDB website was used to predict potential target drugs for hub genes. Reverse transcription-quantitative (RT-q) PCR was employed to detect the expression of these ferroptosis-related genes in clinical samples obtained from healthy controls and patients with CD. According to the two GEO datasets, 13 ferroptosis DEGs (11 upregulated genes and two downregulated genes) were identified in CD with thresholds of $P < 0.05$ and $|\log_2 \text{fold change}| > 1$, and were selected for further analysis. PPI analysis indicated the mutual effects among these genes and filtered out five hub genes. The top 10 potential targeted drugs were selected. The qPCR results showed that the expression levels of three

genes, namely, IL-6, prostaglandin-endoperoxide synthase 2 (PTGS2) and dual oxidase 2 (DUOX2), were different between CD samples and healthy samples. This result was consistent with the results obtained from the bioinformatics analysis. In conclusion, bioinformatics analysis identified a total of 13 ferroptosis-associated genes in CD. Further verification by qPCR showed that IL-6, PTGS2 and DUOX2 may affect the process of CD by regulating ferroptosis. These findings might provide new biomarkers, diagnostic and therapeutic markers for CD.

Introduction

Inflammatory bowel diseases (IBDs) are recognized as chronic inflammatory disorders of the gastrointestinal tract, and include ulcerative colitis (UC) and Crohn's disease (CD) (1). Notably, the global incidence of CD has been on the rise in recent years. Over the past six decades in Western countries, the incidence of CD has gradually risen to 50-200/100,000 individuals. In some other countries with fewer reported cases of CD, such as Japan and South Korea, there has also been a trend of increasing incidence (2,3). CD typically manifests in the terminal ileum, with invasion into the surrounding intestinal tissues (4). In addition, CD carries a predisposition for dysplasia and colorectal cancer (CRC) development (5), with a ~22% risk of cancer development in patients with long-standing CD (6). Furthermore, the manifestations of CD commonly emerge in the advanced stages, frequently with patients already presenting severe intestinal lesions when symptoms become evident (2). Current therapeutic approaches include surgical resection, administration of anti-inflammatory medications or immunosuppressants (2). However, the outcomes have been somewhat unsatisfactory, as a majority of patients encounter short-term recurrence (7).

Ferroptosis, a newly discovered form of programmed cell death, has been implicated in various benign and malignant diseases of the digestive system (8); however, the mechanisms underlying CD associated with ferroptosis-related genes remain incompletely understood. Ferroptosis is a form of cell death that differs from apoptosis and pyroptosis. The main causes are lipid peroxidation, iron accumulation and cell membrane breakdown (9). Furthermore, it has been reported that ferroptosis can participate in the regulation of IBD (10).

Correspondence to: Professor Dianliang Zhang or Dr Hongbo Li, Department of The First General Surgery, Qingdao Hospital, University of Health and Rehabilitation Sciences (Qingdao Municipal Hospital), 1 Jiaozhou Road, Qingdao, Shandong 266011, P.R. China

E-mail: lihongboqingdao@163.com

E-mail: qdslyzdl@126.com

*Contributed equally

Key words: Crohn's disease, ferroptosis, bioinformatics analysis, gene expression

Although ferroptosis is strongly associated with certain digestive tract-related diseases, the mechanisms involved in ferroptosis associated with CD are not understood. Therefore, ferroptosis-related genes in CD were searched for in order to determine the association between CD and ferroptosis. GSE102133 and GSE75214 were used as target datasets to identify differentially expressed genes (DEGs) in CD and these genes were cross-compared with ferroptosis-related genes to determine the object of study. The present study provided new insights into the relationship between CD and ferroptosis, and may provide novel biomarkers for further study in CD research to validate their potential effect on clinical diagnosis and treatment.

Materials and methods

Source of data acquisition. CD-related microarray sequencing datasets were searched in the Gene Expression Omnibus (GEO) database (<https://www.ncbi.nlm.nih.gov/geo/>) for analysis in the present study; the key word was 'crohn disease'. The following screening criteria were used: i) samples from human tissues; ii) the dataset contained microarray expression data; iii) the dataset was acquired from CD ileal mucosa and healthy ileal mucosa; iv) the total number of samples was >10; and v) the number of DEGs was >100. In this manner, two GEO datasets, GSE75214 and GSE102133 (11,12), were enrolled in the present study. These two datasets were based on the GPL6244 platform (Affymetrix Human Gene 1.0 ST Array; Affymetrix; Thermo Fisher Scientific, Inc.); GSE102133 included 65 patients with CD and 12 controls, and GSE75214 contained 67 patients with CD and 11 controls. Specific information regarding the two GSE datasets is shown in Table I. Ferroptosis-related genes were obtained from the FerrDb website (<http://www.zhounan.org/ferrdb/index.html>), and 259 genes were found. The overall research process of the present study is shown in Fig. 1.

Identification of ferroptosis-related DEGs in CD. All microarray data were obtained from the GEO database and the extracted data were normalized by log₂ transformation. Probes were converted to gene symbols according to the annotation information for the normalized data in the platform. A principal component analysis (PCA) plot was generated between the two datasets. Data were standardized using the Limma toolkit (<https://bioconductor.org/packages/release/bioc/html/limma.html>) in R software (version 4.1.2; <http://www.R-project.org/>). |Log₂ fold change (FC)|>1 and P<0.05 were used as the criteria for differential gene expression. The heatmap and volcano plot were drawn using the 'ComplexHeatmap' (<https://bioconductor.org/packages/release/bioc/html/ComplexHeatmap.html>) and 'ggplot2' (<https://ggplot2.tidyverse.org/>) packages in R software. The DEGs were intersected with ferroptosis-related genes from FerrDb, and a Venn diagram was generated using the online Bioinformatics tool (<http://bioinformatics.psb.ugent.be/webtools/Venn/>).

Gene Ontology (GO) functional enrichment and Kyoto Encyclopedia of Genes and Genomes (KEGG) pathway analyses. To further investigate the biological function of the genes involved, GO enrichment analysis was performed, which

included biological process (BP), molecular function (MF) and cellular component (CC), and KEGG pathway enrichment analysis (13-15) was conducted to evaluate related functions. The R package 'clusterProfiler' (<https://bioconductor.org/packages/release/bioc/html/clusterProfiler.html>) toolkit in R software was used for these calculations. P<0.05 was considered to indicate a significant difference. The chord diagram of GO enrichment terms was generated using the circlize R package (version 0.4.1; <https://cran.r-project.org/web/packages/circlize/index.html>). Gene correlation analysis was performed using the Pearson correlation test to assess reciprocal relationships at the mRNA level in CD.

Constructing a protein-protein interaction (PPI) network and hub gene selection. To further investigate the interactions between DEG proteins, PPI network analysis was performed using the Search Tool for the Retrieval of Interacting Genes (STRING) database (<https://string-db.org/>). The PPI network analysis map was visualized by Cytoscape software (version 3.9.1; <https://cytoscape.org/>). First, the STRING database was used to establish the PPI network according to the DEGs, after which the analysis results were exported to Cytoscape for mapping. Nodes represent proteins, lines represent interactions between proteins and different colors represent different functions. Hub genes were obtained from the cytoHubba plugin (<https://apps.cytoscape.org/apps/cytohubba>) in Cytoscape (version 3.9.1) through maximal clique centrality methods. The GeneMANIA website (<https://genemania.org/>) was used for coexpression, physical interaction, colocalization, pathway and other analyses of the five hub genes.

Potential target drug prediction. To predict potential targeted drugs for the five hub genes of CD, predictive analysis was conducted using the DSigDB database. DSigDBv1.0 (<http://dsigdb.tanlab.org/DSigDBv1.0/>) was used to predict the potential targeted drugs for the five hub genes, and the top 10 scores were selected as candidate drugs.

CD and control samples from patients. For the present study, a total of six tissue samples were chosen from the biobank of Qingdao Municipal Hospital (Qingdao, China). Samples were collected from patients between October 2021 and September 2022 and stored in the biobank, and subsequently retrieved for experiments performed in the present study. This comprised three specimens of CD tissue and three specimens of normal intestinal tissue. The use of samples was granted permission by the biobank. Written informed consent was obtained from the patients for inclusion of their samples in the biobank. The research protocol and utilization of samples were both approved and formally authorized by the Ethics Committee of Qingdao Municipal Hospital (Qingdao, China) in October 2022. RT-qPCR was completed in October 2022, and western blotting was completed in November 2023 (approval no. 2022-066).

Hematoxylin and eosin (H&E) staining. All of the tissues were fixed in 10% buffered formalin for 48 h at 4°C, embedded in paraffin and sectioned at a thickness of 4 μm. The slides were then dewaxed twice in 100% xylene for 30 min at 56°C and rehydrated through graded alcohol solutions

Table I. GEO dataset information.

Variable	GEO dataset	
	GSE75214	GSE102133
Platform	GPL6244	GPL6244
Organism	<i>Homo sapiens</i>	<i>Homo sapiens</i>
Contributor(s)	Vancamelbeke <i>et al</i> , 2017 (11)	Verstockt <i>et al</i> , 2019 (12)
Organization name	TARGID-IBD Leuven, Clinical and Experimental Medicine of KU Leuven	KU Leuven
Sample site	Terminal ileum	Ileal mucosal biopsies
Sample number (Crohn's disease and control)	78 (67 CD and 11 Control)	77 (65 CD and 12 Control)
Last update	July 26, 2018	July 25, 2021

CD, Crohn's disease; GEO, Gene Expression Omnibus.

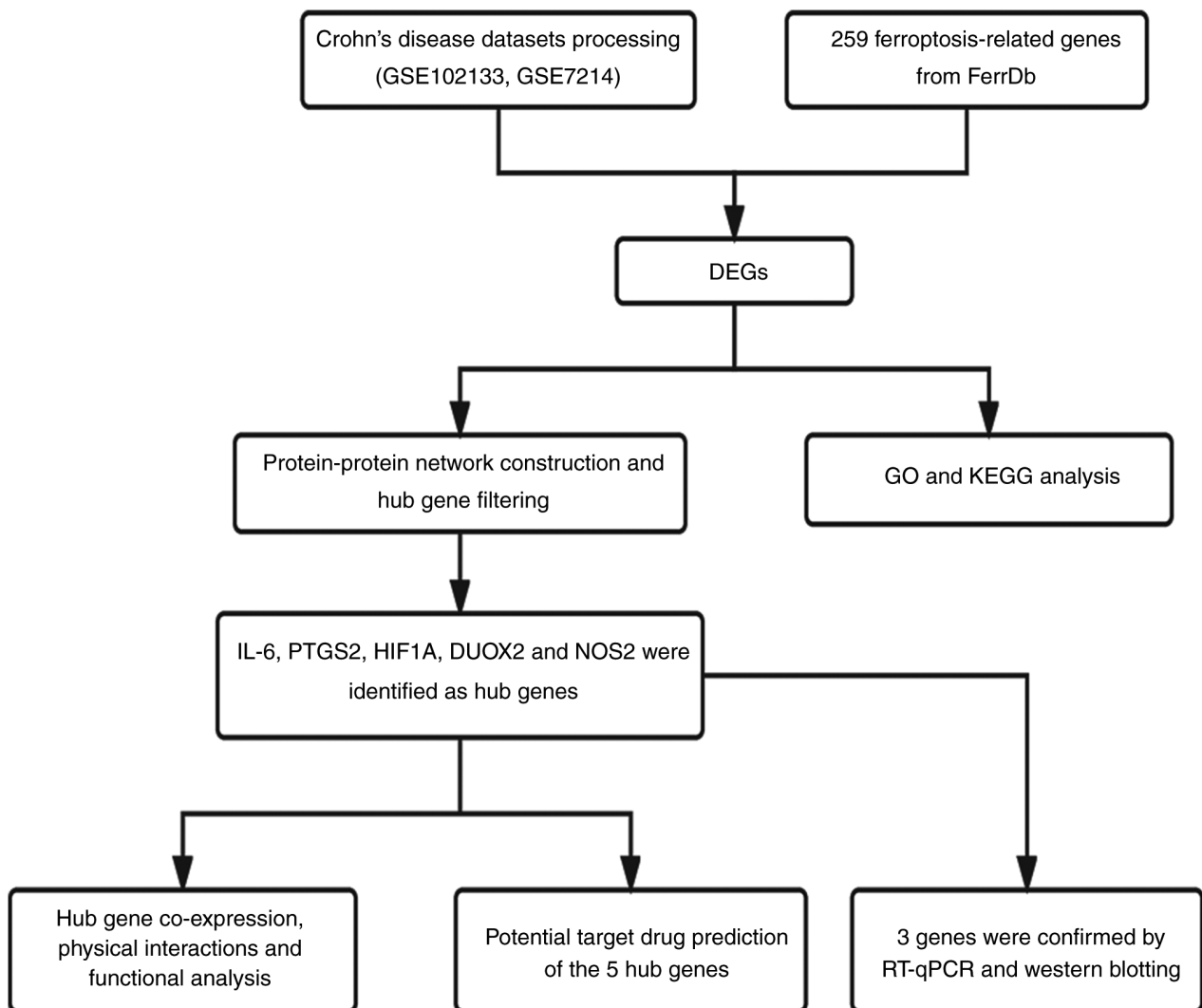


Figure 1. Flow chart of the present study, including data collection, filtering, processing and analysis. DEGs, differentially expressed genes; GO, Gene Ontology; KEGG, Kyoto Encyclopedia of Genes and Genomes; RT-qPCR, reverse transcription-quantitative PCR.

(100, 90, 80, 70 and 50%). The slides were then rinsed in H₂O for 5 min, stained with H&E (cat. no. C0105S; Beyotime Institute of Biotechnology) for 10 min at room temperature,

serially dehydrated in ethanol, cleared in 100% xylene and mounted with a coverslip using Permount (Wuhan Servicebio Technology Co., Ltd.) at room temperature. Finally, the

Table II. Primer sequences.

Gene	Sequence, 5'-3'	RefSeq	Amplicon size, bp
IL-6-F	ACTCACCTCTTCAGAACGAATTG	NG_011640.1	149
IL-6-R	CCATCTTTGGAAGGTTTCAGGTTG		
PTGS2-F	CTGGCGCTCAGCCATACAG	NG_028206.2	94
PTGS2-R	CGCACTTATACTGGTCAAATCCC		
DUOX2-F	CTGGGTCCATCGGGCAATC	NG_009447.1	144
DUOX2-R	GTCGGCGTAATTGGCTGGTA		
HIF1A-F	GAACGTCGAAAAGAAAAGTCTCG	NG_029606.1	124
HIF1A-R	CCTTATCAAGATGCGAACTACA		
NOS2-F	TTCAGTATCACAACTCAGCAAG	NG_011470.1	207
NOS2-R	TGGACCTGCAAGTTAAAATCCC		
GAPDH-F	GGAGCGAGATCCCTCCAAAAT	NG_007073.2	197
GAPDH-R	GGCTGTTGTCATACTTCTCATGG		

F, forward; R, reverse.

sections were imaged under a TE2000 microscope under white light (Nikon Corporation).

RNA isolation and reverse transcription-quantitative PCR (RT-qPCR). A Kz-111-fp high-speed low-temperature grinding instrument (Wuhan Servicebio Technology Co., Ltd.) was used to grind the tissues, and VeZol Reagent (R411-01; Vazyme Biotech Co., Ltd.) was used to extract total RNA. RT to generate cDNA was performed with HiScript II Q Select RT SuperMix (Vazyme Biotech Co., Ltd.) according to the manufacturer's instructions. AceQ Universal SYBR qPCR Master Mix (cat. no. Q511-02; Vazyme Biotech Co., Ltd.) was used for the qPCR analysis process and the reaction was run at 94°C for 3 min, followed by 40 cycles of 94°C for 10 sec and 60°C for 30 sec. All experimental data are presented as the mean values obtained from three independent experiments and were analyzed statistically using the $2^{-\Delta\Delta Cq}$ cycle threshold method (16). Endogenous GAPDH (17) was used as an internal control. All primer sequences are listed in Table II.

Western blotting and antibodies. The tissue grinding method was the same as described in the qPCR section. The ground tissue was lysed using RIPA Lysis Buffer (cat. no. R0010; Beijing Solarbio Science & Technology Co., Ltd.), which contained PMSF (cat. no. P0100; Beijing Solarbio Science & Technology Co., Ltd.), an inhibitor of serine proteases and acetylcholinesterase, on ice. Protein concentration was measured using the BCA Protein Assay kit (cat. no. MA0082; Dalian Meilun Biology Technology Co., Ltd.). The aliquots of lysates (20 μ g protein) were boiled with sample loading buffer (cat. no. LT101S; Epizyme Biotech) for 5 min. Equal amounts of total protein (20 μ g/lane) from different samples were separated by 10% SDS-PAGE at 120 V for 1.5 h and transferred onto 0.22- μ m polyvinylidene difluoride membranes (cat. no. ISEQ00010; MilliporeSigma) at 280 mA for 1.5 h. Then, the membranes were blocked with 5% skimmed milk powder in TBS with 0.05% Tween-20 (TBST) for 1 h at room temperature and treated with specific primary

antibodies overnight at 4°C. The next day, the membranes were washed with TBST and incubated with an HRP-conjugated secondary antibody [1:5,000; cat. nos. SA00001-1 (mouse) and SA00001-2 (rabbit); Proteintech Group, Inc.]. Each band was detected using an enhanced chemiluminescence kit (BeyoECL Star; cat. no. P0018AS; Beyotime Institute of Biotechnology). Anti- β -actin (1:20,000; cat. no. 66009-1-Ig), anti-prostaglandin-endoperoxide synthase 2 (PTGS2)/COX2 (1:1,000; cat. no. 27308-1-AP) and anti-IL-6 (1:1,000; cat. no. 21865-1-AP) were purchased from Proteintech Group, Inc. Anti-dual oxidase 2 (DUOX2; 1:500; cat. no. ab97266) was purchased from Abcam. Antibody Dilution Buffer was purchased from Epizyme Biotech (cat. no. PS119). ImageJ software (version 2.14.0; National Institutes of Health) was used to conduct semi-quantification analysis of blots.

Statistical analysis. R software (version 4.1.2), SPSS 26.0 (IBM Corp.) and Prism 8 (Dotmatics) statistical software were used to perform statistical analysis. In the qPCR experiment, the results were analyzed by unpaired Student's t-test. For the western blot experiment, the results were analyzed by unpaired Student's t-test. Each experiment was repeated three times. $P < 0.05$ was considered to indicate a statistically significant difference.

Results

Analysis of genes associated with ferroptosis in CD. The microarray expression profiling datasets GSE102133 and GSE75214 were downloaded from the GEO database. The present study included a total of 155 samples, consisting of 132 CD samples and 23 control samples. PCA was conducted on the samples from the two GEO datasets. Batch effects identified in the PCA were subsequently removed to ensure data could be further analyzed. The processed PCA plot is presented in Fig. S1A.

Subsequently, $|\log_2 FC| > 1$ and adjusted $P < 0.05$ were used as the criteria to select the DEGs in these two datasets. A volcano plot (Fig. 2A) was generated to display the DEGs between the

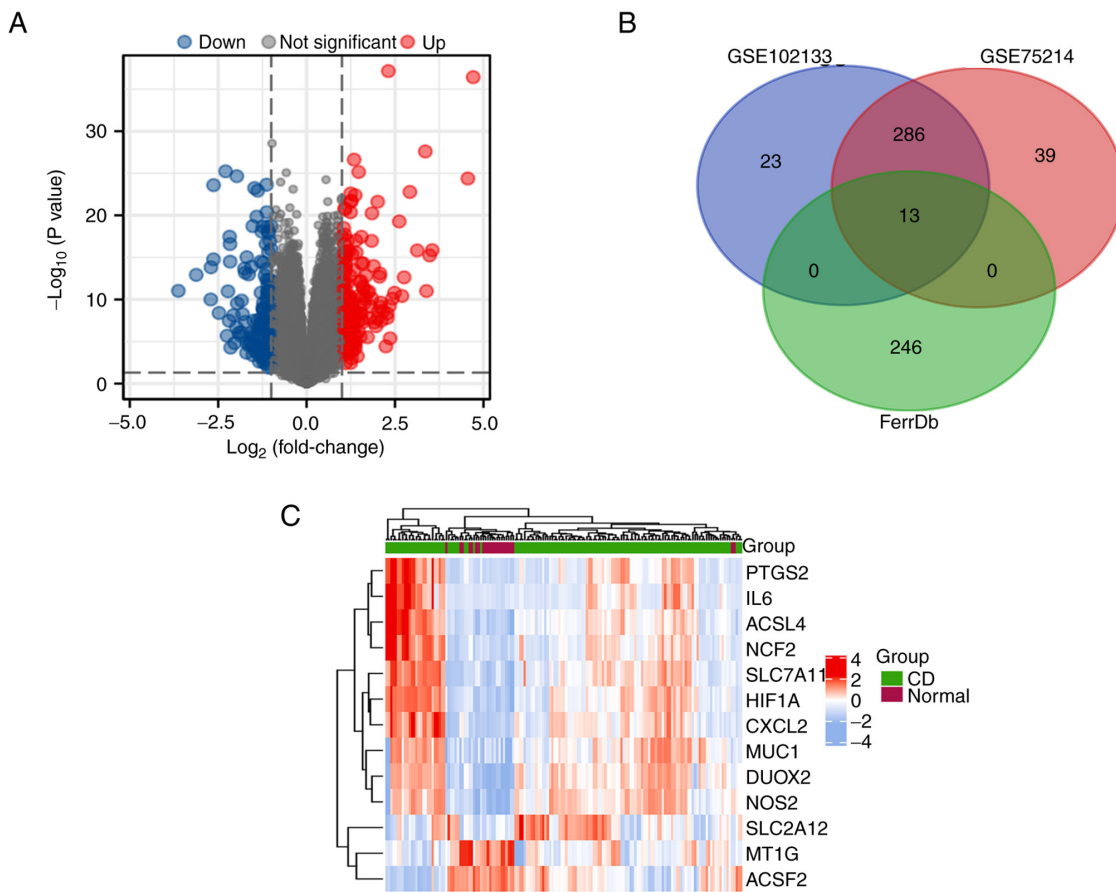


Figure 2. DEGs in the two datasets. (A) Volcano plots of DEGs after removing batch effects for the two datasets; red represents upregulated genes, blue represents downregulated genes; selection criteria are $P < 0.05$, $|\log_2 \text{fold change}| > 1$. (B) Venn diagram demonstrated 13 ferroptosis-related genes detected in the two GSE datasets. (C) Heatmap of 13 differentially expressed ferroptosis-related genes between CD samples and normal samples; red represents upregulated genes, blue represents downregulated genes. CD, Crohn's disease; DEGs, differentially expressed genes.

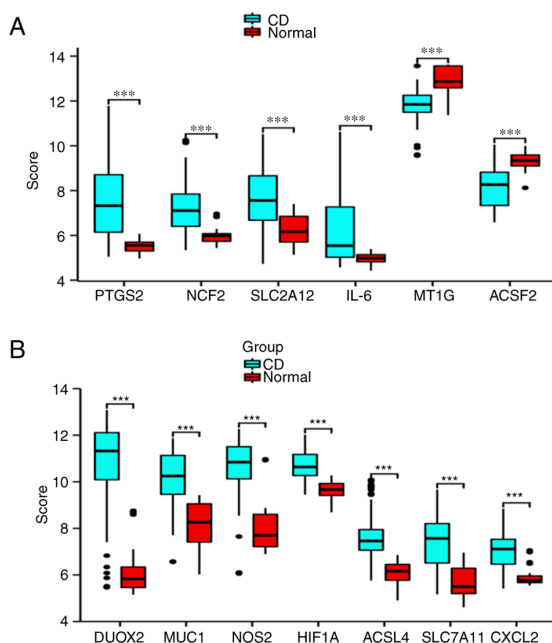


Figure 3. Box plots of the expression of 13 ferroptosis-related genes in CD and normal samples. (A) Expression of PTGS2, NCF2, SLC2A12, IL-6, MT1G and ACSF2. (B) Expression of DUOX2, MUC1, NOS2, HIF1A, ACSL4, SLC7A11 and CXCL2. Blue represents CD group, red represents normal group and the score on the Y-axis represents the relative expression level of genes ($***P < 0.001$). CD, Crohn's disease.

two groups of samples. After performing a crossover analysis with 259 ferroptosis-related genes, a total of 13 DEGs were identified and are shown in a Venn diagram (Fig. 2B). Among these genes, 11 were found to be upregulated, while two were downregulated. A heatmap was generated to illustrate the expression patterns of these genes between the CD group and the normal group (Fig. 2C). The expression levels of the 13 DEGs in the CD samples and normal samples are depicted in box plots (Fig. 3A and B). Significant changes were observed in upregulated genes, including DUOX2 and MUC1, while downregulated genes, such as MT1G and ACSF2, also exhibited significant changes. Detailed information regarding these genes can be found in Table III.

GO enrichment, KEGG pathway and gene interrelationship analyses of DEGs related to ferroptosis in CD. According to the GO enrichment analysis results (Fig. 4A and B), the BP terms that were primarily enriched in the DEGs were 'response to oxidative stress', 'reactive oxygen metabolic process', 'cellular response to oxidative stress' and 'vascular endothelial growth factor production'. The MF and CC terms that were primarily enriched in the DEGs were 'oxidoreductase activity, acting on NAD(P)H' and the 'NADPH oxidase complex'. The KEGG pathway analysis (Fig. 4A) revealed that the enriched genes were predominantly associated with the 'TNF signaling pathway' and the 'IL-17 signaling pathway'. As depicted in the

Table III. Comparison of 13 genes associated with ferroptosis between Crohn's disease samples and normal samples.

Gene symbol	Description	Log fold change	Up/Down regulated	P-value
DUOX2	Dual oxidase 2	4.643206134	Up	4.23×10^{-25}
MUC1	Mucin 1, cell surface associated	2.986183308	Up	1.65188×10^{-23}
NOS2	Nitric oxide synthase 2	2.605279822	Up	5.37157×10^{-20}
HIF1A	Hypoxia inducible factor 1 subunit α	1.055152853	Up	8.37052×10^{-15}
ACSL4	Acyl-CoA synthetase long chain family member 4	1.553297113	Up	6.5226×10^{-13}
SLC7A11	Solute carrier family 7 member 11	1.72699847	Up	1.37298×10^{-11}
CXCL2	C-X-C motif chemokine ligand 2	1.109787323	Up	1.3473×10^{-10}
PTGS2	Prostaglandin-endoperoxide synthase 2	2.034361857	Up	1.76391×10^{-8}
NCF2	Neutrophil cytosolic factor 2	1.213650296	Up	2.63299×10^{-7}
SLC2A12	Solute carrier family 7 member 12	1.23521218	Up	3.29996×10^{-5}
IL-6	Interleukin 6	1.432941749	Up	7.12667×10^{-5}
MT1G	Metallothionein 1G	-1.077752314	Down	1.2887×10^{-11}
ACSF2	Acyl-CoA synthetase family member 2	-1.171871909	Down	9.68187×10^{-9}

Chord diagram generated using the circlize R package (version 0.4.1) of GO enrichment terms (Fig. 4B), the relationships between genes and biological functions within GO are illustrated through connecting lines, with hypoxia inducible factor 1 subunit α (HIF1A), NCF2, PTGS2, nitric oxide synthase 2 (NOS2) and DUOX2 being enriched in multiple GO biological functions.

The Pearson correlation analysis indicated that several of the 13 ferroptosis-related genes exhibited significant positive and negative correlations in CD (Fig. 4C). Red and blue colors represent positive and negative correlations, respectively.

PPI network generation and filtering of hub genes associated with ferroptosis. PPI analysis was conducted to demonstrate the relationships among the genes of interest (Fig. S1B). Out of the 13 genes, three were excluded from the analysis because they did not exhibit any interactions with each other. The remaining 10 genes were used to construct the PPI network. Genes are represented by nodes, and the interactions among the genes are indicated by lines (Fig. 5A). Next, cytoHubba plugin in Cytoscape software identified the following five hub genes: IL-6, PTGS2, HIF1A, DUOX2 and NOS2 (Fig. 5B). The deeper color of the dot indicates that the rank order of the hub gene is more advanced. The GeneMANIA website was used to predict the gene coexpression, functional analysis and physical binding properties of these five hub genes, as illustrated in Fig. 5C. Notably, the coexpressed genes for the five genes were functionally enriched in cellular response to oxygen levels, oxidoreductase activity, acute inflammatory response and other related functions.

Targeted drug prediction for related genes. The DSigDB database was used to predict target drugs associated with the five hub genes, which have the potential to control the occurrence of ferroptosis and treat CD. A total of 1,378 potential drugs were predicted, and among them, zinc protoporphyrin, chitosamine, benzoyl peroxide, ferric citrate and haem were

identified as the top-rated drugs. The specific ratings and statistical values are shown in Table IV.

Validation of the differential expression of the five hub genes in CD clinical samples by RT-qPCR. All collected clinical tissue samples of CD were definitively diagnosed by two pathologists through observation under a colonoscope, tissue sectioning and H&E staining. The clinicopathological features of the patients are shown in Table V. The H&E staining and colonoscopy findings are shown in Fig. 6. Under the microscope, visible infiltration of inflammatory cells and lymphocytes was observed. Colonoscopy indicated that the intestinal lumen exhibited a coarse and congested surface, accompanied by focal mucosal ulceration and numerous irregular protuberant lesions. RT-qPCR analysis was performed to detect the expression levels of the five hub genes in three pairs of CD tissues and healthy control tissues. The statistical analysis revealed significant changes in the expression levels of IL-6, PTGS2 and DUOX2 between the samples. Although the expression patterns of HIF1A and NOS2 were consistent with the bioinformatics analysis results, the difference in their expression between groups was not significant (Fig. 7).

Validation of the protein expression levels of the three genes in CD clinical samples. Protein expression level validation of the three target genes identified through RT-qPCR experiments was conducted in normal and CD tissues using western blotting (Fig. 8A and B). The protein expression level results were in accordance with the qPCR findings.

Discussion

CD is a chronic, long-term and recurring intestinal disease that belongs to a group of conditions collectively known as IBD (18). Prior to the 20th century, the incidence of CD was more prevalent in the Americas and Europe; however, in recent years, there has been a steady rise in the prevalence of CD in Asian countries (19). CD primarily develops in the terminal

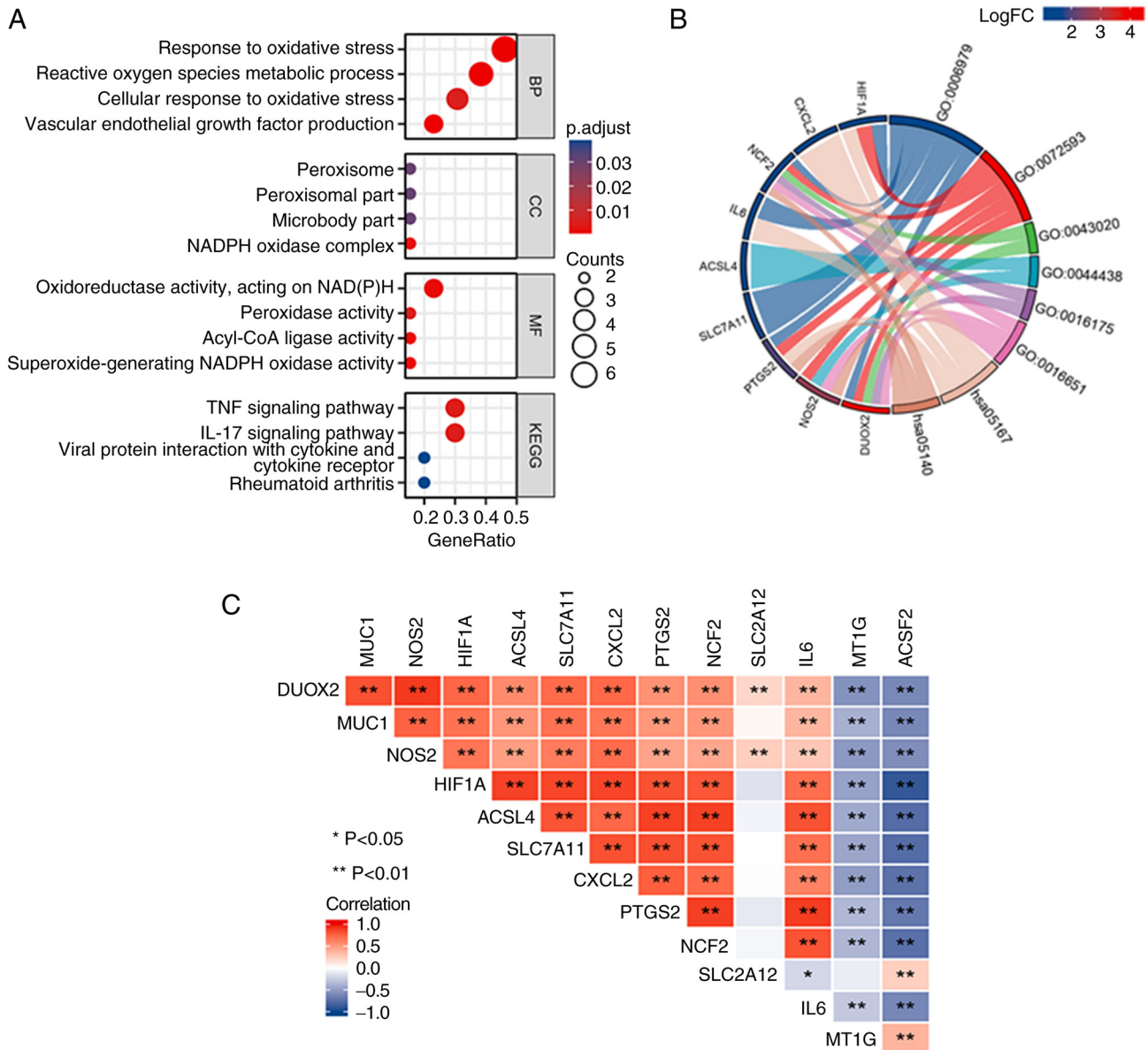


Figure 4. GO enrichment and KEGG pathway analyses of 13 ferroptosis-related genes. (A) Bubble diagram of GO enrichment including BP, CC and MF, and KEGG pathway enrichment. (B) Chord diagram of GO enrichment. Some of genes are not shown because the enrichment lines were too scattered in the plot. (C) Pearson correlation test of 13 ferroptosis-associated genes in Crohn's disease samples and healthy samples. *P<0.05 and **P<0.01. BP, biological process; CC, cellular component; GO, Gene Ontology; KEGG, Kyoto Encyclopedia of Genes and Genome; MF, molecular function.

ileum and can lead to lesions that extend from the mouth to the anus, as well as potential extraintestinal complications. CD often presents subtle or atypical symptoms in a clinical setting, which can pose challenges in its detection and diagnosis. Consequently, patients are frequently overlooked or missed during colonoscopy procedures (20). Patients commonly experience symptoms, such as diarrhea, abdominal pain, fever and anemia. Additionally, CD can present with extraintestinal manifestations, including inflammatory arthropathy, osteoporosis, scleritis and IgA nephropathy (21,22). A review of the PubMed database revealed that the current findings on risk factors for CD include environmental factors, genetic factors, nutritional status, intestinal barrier disorders, immune response, microbial dysbiosis, gut viruses and fungi (3,23). However, the specific mechanisms or pathways involved in these risk factors remain to be elucidated.

Ferroptosis is a recently discovered form of iron-dependent, nonapoptotic cell death that is primarily triggered by intracellular lipid peroxidation. Ferroptosis is regulated by various oxidative and antioxidant systems *in vivo*, including redox homeostasis, mitochondrial activation, amino acid metabolism, lipid metabolism and sugar metabolism (7). Ferroptosis has been observed to regulate various benign or malignant diseases through multiple pathways, such as disrupting cellular metabolic homeostasis, causing mitochondrial damage or activating other cell death pathways. These diseases include but are not limited to tumors, neurological disorders, kidney damage and cardiovascular diseases (24-26).

Huang *et al* (27) indicated that the ferroptosis-related hub gene STAT3 can mediate the process of ferroptosis and promote UC. Ferroptosis also plays a significant role in the regulation of CRC. Glutathione peroxidase 4, an inhibitor

Table IV. Top 10 predicted target drugs based on five hub genes.

Drug name	P-value	Odds ratio	Combined score
Zinc protoporphyrin CTD 00000915	2.74x10 ⁻⁸	1,152.057692	20,062.49288
Chitosamine CTD 00006030	1.66x10 ⁻⁹	959.6144578	19,397.65623
Benzoyl peroxide CTD 00005495	2.75x10 ⁻⁶	1,480.444444	18,956.85145
Ferric citrate CTD 00001186	3.30x10 ⁻⁶	1,332.333333	16,817.52991
Heme TTD 00008407	3.30x10 ⁻⁶	1,332.333333	16,817.52991
Flufenamic acid CTD 00005976	4.48x10 ⁻⁸	966	16,346.25293
Roxithromycin CTD 00007073	3.90x10 ⁻⁶	1,211.151515	15,085.68949
Kaempferol CTD 00000297	3.85x10 ⁻⁹	772.5048544	14,966.43303
NSC267099 CTD 00001568	4.54x10 ⁻⁶	1,110.166667	1,3656.83282
Deferoxamine CTD 00005759	7.00x10 ⁻⁹	641	1,1953.71327

Table V. Clinicopathological characteristics of patients with Crohn's disease.

Characteristic	CD Patient 1	CD Patient 2	CD Patient 3	Control 1	Control 2	Control 3
Age, years	32	53	41	42	38	44
Sex	Female	Male	Female	Male	Male	Female
Sample location	Ileocecal region	Ascending colon	Terminal ileum	Ileocecal region	Terminal ileum	Terminal ileum

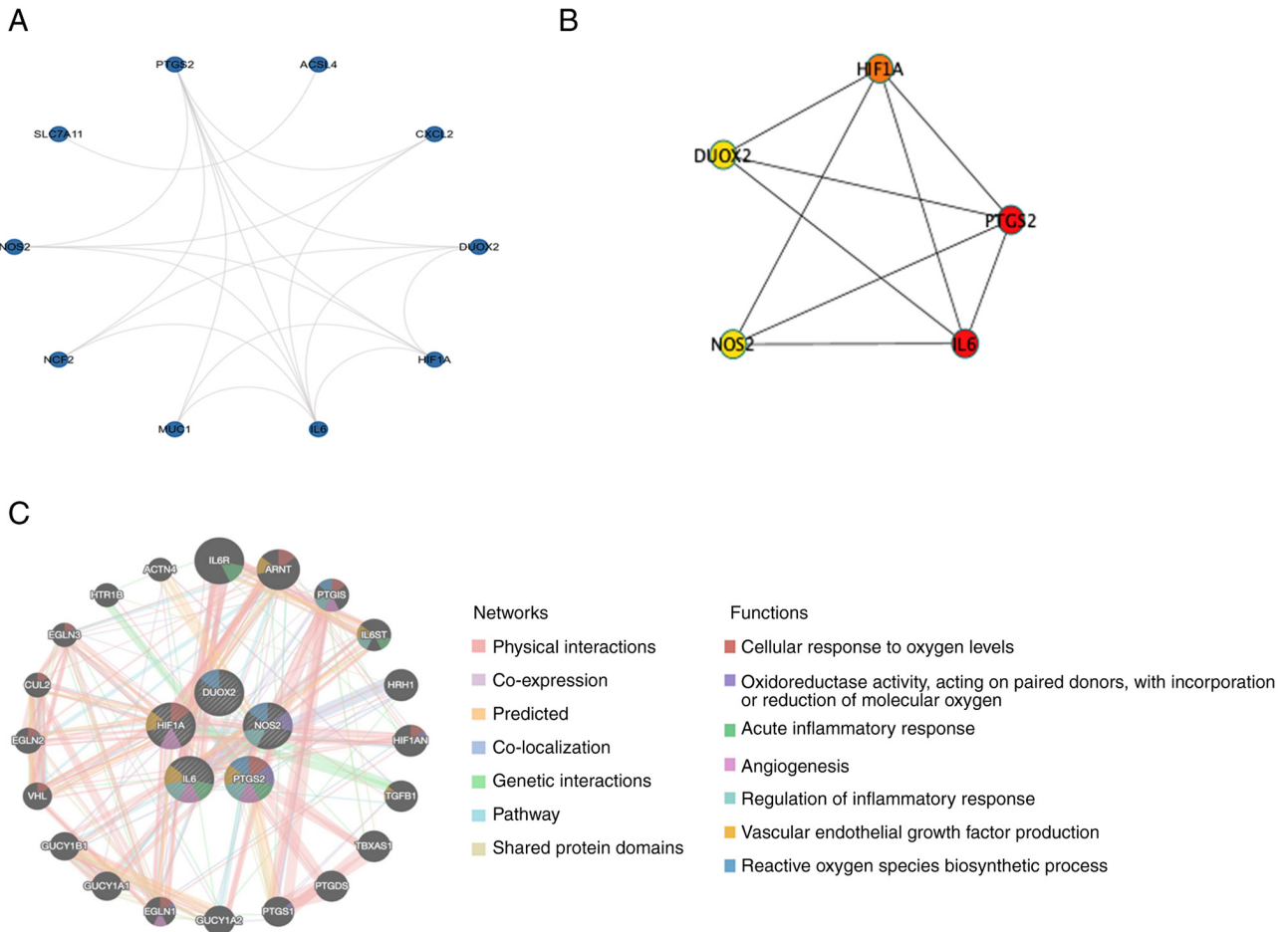


Figure 5. PPI analysis of the interactions between differentially expressed genes. (A) PPI network map of 10 ferroptosis-related genes. (B) The five hub genes calculated from the PPI network. (C) The five hub genes correlation interaction network map, as determined by GeneMANIA. PPI, protein-protein interaction.

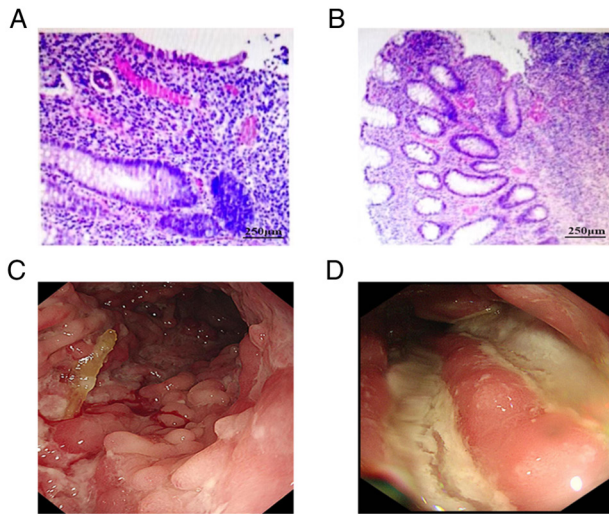


Figure 6. Histopathological results of intestinal tissue biopsies and endoscopic findings of intestinal lesions. (A) Pathological sections reveal infiltration of lymphocytes and inflammatory cells. (B) Pathological sections show chronic inflammatory changes in the mucosa, accompanied by lymphocyte infiltration. Scale bar, 250 μ m. (C) In colonoscopy, the intestinal lumen exhibited a coarse surface, accompanied by numerous irregular protuberant lesions. (D) The mucosal surface of the intestinal lumen was rough, accompanied by congestion and edema.

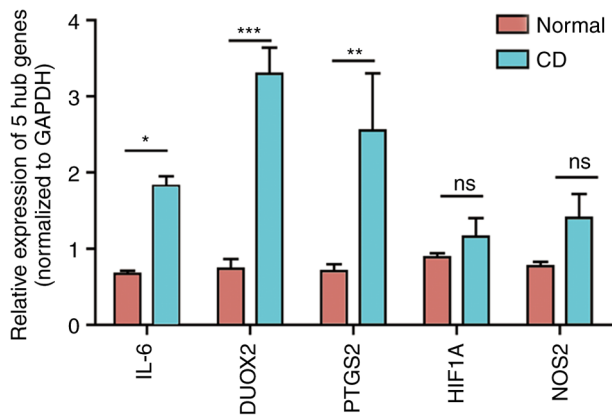


Figure 7. Verification of the expression levels of the five hub candidate genes in clinical tissue samples. Expression levels were normalized to GAPDH as an internal reference and P-values were calculated using the Student's t-test. *P<0.05; **P<0.01; ***P<0.001; ns, not significant; CD, Crohn's disease; DUOX2, dual oxidase 2; HIF1A, hypoxia inducible factor 1 subunit α ; NOS2, nitric oxide synthase 2; PTGS2, prostaglandin-endoperoxide synthase 2.

of ferroptosis, is an important central regulatory molecule involved in the progression of CRC (28).

Regarding the intestinal barrier and immune response, which are key mechanisms contributing to CD, ferroptosis also plays an important role. Liu *et al* (29) discovered that ferroptosis can reverse the maintenance of intestinal mucosal barrier integrity mediated by Sestrin2. Ma *et al* (30) reported that CD36-directed CD8⁺ T-cell ferroptosis suppresses anti-tumor effects *in vivo*. Xu *et al* (31) suggested that ferroptosis could exert anti-tumor effects by reversing the immune micro-environment. For example, CD8⁺ T cells activated during the immune regulation process can induce cellular ferroptosis by promoting lipid peroxidation in cells and finally enhancing

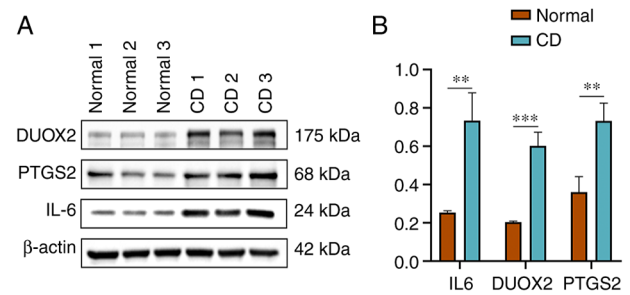


Figure 8. Western blotting was performed to confirm the expression levels of the three target genes from quantitative PCR in clinical tissue samples. The observed expression patterns were consistent with the PCR results and quantification was normalized to β -actin as an internal reference. (A) DUOX2, PTGS2 and IL-6 protein levels in samples. (B) Statistical histogram displaying the variances in the expression levels of the DUOX2, PTGS2 and IL-6 proteins following a semi-quantitative analysis performed using ImageJ software. **P<0.01, ***P<0.001. CD, Crohn's disease; DUOX2, dual oxidase 2; PTGS2, prostaglandin-endoperoxide synthase 2.

its anti-tumor effect. The present study conducted an analysis to investigate the potential interaction between CD and ferroptosis.

Based on the GEO datasets and the FerrDb, a total of 13 DEGs that are associated with ferroptosis were identified. The present study further investigated the functional implications of these genes through GO and KEGG enrichment analyses. The GO analysis indicated that the BPs associated with ferroptosis were related to oxidative stress. These processes include the 'response to oxidative stress', 'reactive oxygen species metabolic process' and 'cellular response to oxidative stress'. This finding suggested that ferroptosis may be implicated in the onset of Crohn's disease, as oxidative stress processes play a crucial role in the occurrence of ferroptosis. The accumulation of iron during cellular metabolism can lead to impaired redox homeostasis, thereby inducing ferroptosis in cells (32,33). Oxidative stress is also an important factor in inflammation, which activates a variety of proinflammatory factors, such as NF- κ B and p53 (34). The increased expression of p53 in CD has been shown to promote apoptosis of intestinal epithelial cells and aggravate inflammation (35,36). Therefore, it was hypothesized that the oxidative stress process associated with the ferroptosis pathway might be implicated in the occurrence and progression of CD.

Another noteworthy result obtained in terms of BP enrichment specifically related to 'vascular endothelial growth factor production'. Vascular endothelial growth factor (VEGF) is a biomolecule that is crucial for mitosis and preventing apoptosis in vascular endothelial cells (37) and includes several members, including VEGF-A, VEGF-B and VEGF-C. Inflammation and tumors typically promote pathological vascular proliferation, leading to an increased oxygen demand in the local microenvironment (38). The concentration of reactive oxygen species (ROS) that depends on the production of NADPH oxidase during pathological vascular proliferation also increases, which appears to establish a reciprocal relationship with ferroptosis (39). High production of ROS increases the likelihood of ferroptosis in cells (40). This is also consistent with the enrichment results obtained for MF) and CC.

In other studies, the biomodulatory role of VEGF in IBD has been reported. Scaldaferri *et al* (41) reported that overexpression of VEGF-A in mice with DSS-induced IBD inflammation can exacerbate disease severity. According to Eder *et al* (42), the degree of VEGF expression can affect the severity of CD. However, the existing mechanism between VEGF and ferroptosis remains to be elucidated. It was hypothesized that VEGF may lead to ferroptosis of intestinal epithelial cells and promote the occurrence of CD.

KEGG pathway analysis further revealed that the relevant genes were predominantly abundant in the 'TNF pathway', 'IL-17 pathway' and 'rheumatoid arthritis'. TNF is an important cell regulatory molecule involved in the regulation of cell survival, apoptosis, inflammation and the immune response (43). IL-7 is an inflammatory factor secreted by T helper 17 cells (44). Bishu *et al* (45) detected elevated expression levels of both TNF and IL-17 in CD, which may be associated with a type of CD4⁺ T cells referred to as CD4⁺ tissue-resident memory T cells (TRM cells). CD4⁺ TRM cells proliferate in CD and serve as the primary sources of TNF and IL-17. However, the regulatory relationship between ferroptosis and TNF and IL-17 in the currently available studies of CD remains to be elucidated.

A PPI network map was generated in Cytoscape and five hub genes, IL-6, PTGS2, HIF1A, DUOX2 and NOS2, were identified using cytoHubba software. Subsequently, RT-qPCR and western blotting experiments were conducted on three pairs of patient samples to analyze the expression of these genes. The results demonstrated significant differences in the expression levels of IL-6, DUOX2 and PTGS2.

IL-6 is an inflammatory cytokine belonging to the IL family. It serves a crucial role in stimulating anti-inflammatory processes and immune responses in the human body (46). Shi *et al* (47) suggested that Toll-like receptor 4 aggravates intestinal injury by regulating the expression of IL-6. Gross *et al* (48) identified significantly elevated IL-6 in CD in both the active and inactive phases. IL-6 plays a role in other processes besides inflammation. Han *et al* (49) revealed that, in asthma, IL-6 disrupts iron homeostasis in BEAS-2B cells by promoting lipid peroxidation, which in turn promotes ferroptosis in bronchial epithelial cells. Li *et al* (50) recently demonstrated that the expression of an amino acid counter transporter (xCT) in head and neck squamous cell carcinoma was associated with the levels of IL-6 and that xCT can induce cellular ferroptosis. These findings indirectly confirm that IL-6 can regulate ferroptosis by promoting lipid peroxidation, thereby exacerbating the severity of inflammation. However, there is no conclusive evidence for an association between IL-6 and ferroptosis in CD, and further study is required to determine the specific mechanism between IL-6 and ferroptosis in CD.

PTGS2, also called COX-2, is an enzyme that can be suppressed by nonsteroidal anti-inflammatory drugs, such as aspirin and ibuprofen, and serves a regulatory role in a number of inflammatory or neoplastic diseases (51). Roberts *et al* (52) revealed through densitometric analysis that the expression of COX-2 was increased by 6-8 times in IBD tissues compared with normal tissues. Singer *et al* (53) demonstrated that COX-2 was predominantly present in apical epithelial cells and in lamina propria mononuclear cells in CD. Notably, neither study detected COX-2 expression in normal tissues. Furthermore, it has been confirmed in the literature that COX-2-induced

ferroptosis may be associated with heme oxygenase (HO)-1, which has been identified as a crucial mediator of ferroptosis (54). Chen *et al* (55) discovered that the use of astragalus polysaccharides, by inhibiting HO-1 expression, can treat ferroptosis and reduce COX-2 expression. It was hypothesized that there may be a certain interaction between COX-2 and HO-1, thereby regulating the relationship between CD and ferroptosis. These results suggested that PTGS2/COX-2 may have an important regulatory role in CD. However, to the best of our knowledge, no related research has determined whether the upregulation of COX-2 in CD is associated with ferroptosis. This notion provides a foundation for future mechanistic studies on the occurrence of CD.

DUOX2 is an enzyme that was initially discovered in the mammalian thyroid and belongs to the NADPH oxidase family, responsible for the production of ROS. ROS are an important component of the immune system in eukaryotic organisms. However, excessive levels of ROS in cells may induce and promote ferroptosis. Lipinski *et al* (56) demonstrated that DUOX2 is an important factor involved in NOD2-dependent ROS production. A separate study on pediatric CD conducted by Haberman *et al* (57) observed strong and robust expression of DUOX2 in the villous enterocytes of the ileum affected by CD. This increased expression of DUOX2 could potentially contribute to the worsening of intestinal mucosal damage. This finding seems to further support the hypothesis of the present study that the upregulation of DUOX2 in intestinal mucosal cells may have a role in the pathogenesis of CD. The increased expression of DUOX2 in the villous enterocytes of the small intestine could lead to the accumulation of ROS within the cells, consequently promoting iron-mediated cell death and resulting in the loss of intestinal mucosal barrier function.

Current treatment options for CD are typically limited to anti-inflammatory medications, immunosuppressive agents and surgical interventions. However, the treatment outcomes are often unsatisfactory, with high rates of recurrence and severe side effects (58,59). Based on the results of the present study, drug targets for the five hub genes were inferred using the DSigDB database. Based on existing research on the target drugs, kaempferol was found to inhibit the initiation of cellular ferroptosis. Additionally, other studies have shown that kaempferol can be used to improve intestinal inflammation and intestinal barrier disorders (60,61).

The present study has several limitations. First, the datasets used in the present study were obtained from the GEO database and both datasets were generated using the same microarray platform. In addition, there was a lack of additional validation through cell or animal experiments, as well as clinical validation. Moreover, the number of tissue samples obtained for clinical experiments and testing was relatively small. Therefore, further investigations are needed in future studies to explore the relationship between ferroptosis and CD.

In conclusion, 13 ferroptosis-associated genes were identified in CD in the present bioinformatics analysis. Among them, IL-6, DUOX2 and PTGS2 may be most likely to regulate ferroptosis in CD, and to be involved in CD development and progression. However, specific mechanistic studies need to be further explored. These results provide an experimental foundation for targeted therapy in CD, introducing novel ideas, insights and methods for understanding the development and occurrence of CD.

Acknowledgements

Not applicable.

Funding

The present study was financially supported by the National Natural Science Foundation of China (grant nos. 81270448 and 81470890).

Availability of data and materials

The datasets generated and/or analyzed during the current study are available in the GEO repository, <https://www.ncbi.nlm.nih.gov/geo/query/acc.cgi?acc=GSE102133> and <https://www.ncbi.nlm.nih.gov/geo/query/acc.cgi?acc=GSE75214>. Other datasets used and/or analyzed during the current study are available from the corresponding authors on reasonable request.

Authors' contributions

WZ, ZL, HL and DZ contributed to the study conception and design. Material preparation, data collection and analysis were performed by WZ and ZL. HL and ZL confirm the authenticity of all the raw data. The first draft of the manuscript was written by WZ and all authors commented on previous versions of the manuscript. HL conceived the concept, designed the manuscript, coordinated and critically revised the manuscript. DZ provided valuable suggestions and assistance during the revision processes of the manuscript, offered financial support for the experiments and collaborated with all authors to finalize the content of the manuscript. All authors read and approved the final manuscript.

Ethics approval and consent to participate

The present study was performed in line with the principles of The Declaration of Helsinki. Approval was granted by the Ethics Committee of Qingdao Municipal Hospital (approval no. 2022-066). Written informed consent was obtained from the patients for inclusion of their samples in the biobank.

Patient consent for publication

Not applicable.

Competing interests

The authors declare that they have no competing interests.

References

- Geremia A, Biancheri P, Allan P, Corazza GR and Di Sabatino A: Innate and adaptive immunity in inflammatory bowel disease. *Autoimmun Rev* 13: 3-10, 2014.
- Cosnes J, Gower-Rousseau C, Seksik P and Cortot A: Epidemiology and natural history of inflammatory bowel diseases. *Gastroenterology* 140: 1785-1794, 2011.
- Roda G, Chien Ng S, Kotze PG, Argollo M, Panaccione R, Spinelli A, Kaser A, Peyrin-Biroulet L and Danese S: Crohn's disease. *Nat Rev Dis Primer* 6: 22, 2020.
- Dulai PS, Singh S, Vande Castele N, Boland BS, Rivera-Nieves J, Ernst PB, Eckmann L, Barrett KE, Chang JT and Sandborn WJ: Should we divide Crohn's disease into ileum-dominant and isolated colonic diseases? *Clin Gastroenterol Hepatol* 17: 2634-2643, 2019.
- Friedberg S and Rubin DT: Intestinal cancer and dysplasia in Crohn's disease. *Gastroenterol Clin North Am* 51: 369-379, 2022.
- Friedman S: Cancer in Crohn's disease. *Gastroenterol Clin North Am* 35: 621-639, 2006.
- Baumgart DC and Sandborn WJ: Crohn's disease. *Lancet* 380: 1590-1605, 2012.
- Jiang X, Stockwell BR and Conrad M: Ferroptosis: Mechanisms, biology and role in disease. *Nat Rev Mol Cell Biol* 22: 266-282, 2021.
- Li J, Cao F, Yin HL, Huang ZJ, Lin ZT, Mao N, Sun B and Wang G: Ferroptosis: Past, present and future. *Cell Death Dis* 11: 88, 2020.
- Xu C, Liu Z and Xiao J: Ferroptosis: A double-edged sword in gastrointestinal disease. *Int J Mol Sci* 22: 12403, 2021.
- Vancamelbeke M, Vanuytsel T, Farré R, Verstockt S, Ferrante M, Van Assche G, Rutgeerts P, Schuit F, Vermeire S, Arijis I and Cleynen I: Genetic and transcriptomic bases of intestinal epithelial barrier dysfunction in inflammatory bowel disease. *Inflamm Bowel Dis* 23: 1718-1729, 2017.
- Verstockt S, De Hertogh G, Van der Goten J, Verstockt B, Vancamelbeke M, Machiels K, Van Lommel L, Schuit F, Van Assche G, Rutgeerts P, *et al*: Gene and miRNA regulatory networks during different stages of Crohn's disease. *J Crohns Colitis* 13: 916-930, 2019.
- Kanehisa M, Furumichi M, Sato Y, Kawashima M and Ishiguro-Watanabe M: KEGG for taxonomy-based analysis of pathways and genomes. *Nucleic Acids Res* 51: D587-D592, 2023.
- Kanehisa M and Goto S: KEGG: Kyoto encyclopedia of genes and genomes. *Nucleic Acids Res* 28: 27-30, 2000.
- Kanehisa M: Toward understanding the origin and evolution of cellular organisms. *Protein* 28: 1947-1951, 2019.
- Livak KJ and Schmittgen TD: Analysis of relative gene expression data using real-time quantitative PCR and the 2(-Delta Delta C(T)) method. *Methods* 25: 402-408, 2001.
- Yao B, Zhang Q, Yang Z, An F, Nie H, Wang H, Yang C, Sun J, Chen K, Zhou J, *et al*: CircEZH2/miR-133b/IGF2BP2 aggravates colorectal cancer progression via enhancing the stability of m6A-modified CREB1 mRNA. *Mol Cancer* 21: 140, 2022.
- Veauthier B and Hornecker JR: Crohn's disease: Diagnosis and management. *Am Fam Physician* 98: 661-669, 2018.
- Chiba M, Morita N, Nakamura A, Tsuji K and Harashima E: Increased incidence of inflammatory bowel disease in association with dietary transition (westernization) in Japan. *JMA J* 4: 347-357, 2021.
- Chetcuti Zammit S, Ellul P and Sidhu R: The role of small bowel endoscopy for Crohn's disease. *Curr Opin Gastroenterol* 35: 223-234, 2019.
- Wilkins T, Jarvis K and Patel J: Diagnosis and management of Crohn's disease. *Am Fam Physician* 84: 1365-1375, 2011.
- Ambruzs JM and Larsen CP: Renal manifestations of inflammatory bowel disease. *Rheum Dis Clin North Am* 44: 699-714, 2018.
- Prieto JMI, Andrade AR, Magro DO, Imbrizi M, Nishitokukado I, Ortiz-Agostinho CL, Dos Santos FM, Luzia LA, Rondo PHC, Leite AZA, *et al*: Nutritional global status and its impact in Crohn's disease. *J Can Assoc Gastroenterol* 4: 290-295, 2021.
- Wu X, Li Y, Zhang S and Zhou X: Ferroptosis as a novel therapeutic target for cardiovascular disease. *Theranostics* 11: 3052-3059, 2021.
- Mahoney-Sánchez L, Bouchaoui H, Ayton S, Devos D, Duce JA and Devedjian JC: Ferroptosis and its potential role in the pathophysiology of Parkinson's disease. *Prog Neurobiol* 196: 101890, 2021.
- Martin-Sanchez D, Fontecha-Barriuso M, Martinez-Moreno JM, Ramos AM, Sanchez-Niño MD, Guerrero-Hue M, Moreno JA, Ortiz A and Sanz AB: Ferroptosis and kidney disease. *Nefrologia (Engl Ed)* 40: 384-394, 2020 (In English, Spanish).
- Huang F, Zhang S, Li X, Huang Y, He S and Luo L: STAT3-mediated ferroptosis is involved in ulcerative colitis. *Free Radic Biol Med* 188: 375-385, 2022.
- Sui X, Zhang R, Liu S, Duan T, Zhai L, Zhang M, Han X, Xiang Y, Huang X, Lin H and Xie T: RSL3 drives ferroptosis through GPX4 inactivation and ROS production in colorectal cancer. *Front Pharmacol* 9: 1371, 2018.

29. Liu W, Xu C, Zou Z, Weng Q and Xiao Y: Sestrin2 suppresses ferroptosis to alleviate septic intestinal inflammation and barrier dysfunction. *Immunopharmacol Immunotoxicol* 45: 123-132, 2023.
30. Ma X, Xiao L, Liu L, Ye L, Su P, Bi E, Wang Q, Yang M, Qian J and Yi Q: CD36-mediated ferroptosis dampens intratumoral CD8⁺ T cell effector function and impairs their antitumor ability. *Cell Metab* 33: 1001-1012.e5, 2021.
31. Xu H, Ye D, Ren M, Zhang H and Bi F: Ferroptosis in the tumor microenvironment: Perspectives for immunotherapy. *Trends Mol Med* 27: 856-867, 2021.
32. Yu Y, Yan Y, Niu F, Wang Y, Chen X, Su G, Liu Y, Zhao X, Qian L, Liu P and Xiong Y: Ferroptosis: A cell death connecting oxidative stress, inflammation and cardiovascular diseases. *Cell Death Discov* 7: 193, 2021.
33. Mancardi D, Mezzanotte M, Arrigo E, Barinotti A and Roetto A: Iron overload, oxidative stress, and ferroptosis in the failing heart and liver. *Antioxidants (Basel)* 10: 1864, 2021.
34. Reuter S, Gupta SC, Chaturvedi MM and Aggarwal BB: Oxidative stress, inflammation, and cancer: How are they linked? *Free Radic Biol Med* 49: 1603-1616, 2010.
35. Gu L, Ge Z, Wang Y, Shen M and Zhao P: Activating transcription factor 3 promotes intestinal epithelial cell apoptosis in Crohn's disease. *Pathol Res Pract* 214: 862-870, 2018.
36. Zhang J, Xu M, Zhou W, Li D, Zhang H, Chen Y, Ning L, Zhang Y, Li S, Yu M, *et al*: Deficiency in the anti-apoptotic protein DJ-1 promotes intestinal epithelial cell apoptosis and aggravates inflammatory bowel disease via p53. *J Biol Chem* 295: 4237-4251, 2020.
37. Melincovici CS, Boşca AB, Şuşman S, Mărginean M, Mihu C, Istrate M, Moldovan IM, Roman AL and Mihu CM: Vascular endothelial growth factor (VEGF)-key factor in normal and pathological angiogenesis. *Rom J Morphol Embryol* 59: 455-467, 2018.
38. Kvietys PR and Granger DN: Role of reactive oxygen and nitrogen species in the vascular responses to inflammation. *Free Radic Biol Med* 52: 556-592, 2012.
39. Fukai T and Ushio-Fukai M: Cross-talk between nadph oxidase and mitochondria: Role in ros signaling and angiogenesis. *Cells* 9: 1849, 2020.
40. Su LJ, Zhang JH, Gomez H, Murugan R, Hong X, Xu D, Jiang F and Peng ZY: Reactive oxygen species-induced lipid peroxidation in apoptosis, autophagy, and ferroptosis. *Oxid Med Cell Longev* 2019: 5080843, 2019.
41. Scaldaferrri F, Vetrano S, Sans M, Arena V, Straface G, Stigliano E, Repici A, Sturm A, Malesci A, Panes J, *et al*: VEGF-A links angiogenesis and inflammation in inflammatory bowel disease pathogenesis. *Gastroenterology* 136: 585-95.e5, 2009.
42. Eder P, Korybalska K, Lykowska-Szuber L, Krela-Kazmierczak I, Stawczyk-Eder K, Klimczak K, Szymczak A, Linke K and Witowski J: Association of serum VEGF with clinical response to anti-TNF α therapy for Crohn's disease. *Cytokine* 76: 288-293, 2015.
43. Bradley JR: TNF-mediated inflammatory disease. *J Pathol* 214: 149-160, 2008.
44. Iwakura Y, Ishigame H, Saijo S and Nakae S: Functional specialization of interleukin-17 family members. *Immunity* 34: 149-162, 2011.
45. Bishu S, El Zaatari M, Hayashi A, Hou G, Bowers N, Kinnucan J, Manoogian B, Muza-Moons M, Zhang M and Grasberger H, *et al*: CD4⁺ tissue-resident memory T cells expand and are a major source of mucosal tumour necrosis factor α in active Crohn's disease. *J Crohns Colitis* 13: 905-915, 2019.
46. Tanaka T, Narazaki M and Kishimoto T: IL-6 in inflammation, immunity, and disease. *Cold Spring Harb Perspect Biol* 6: a016295, 2014.
47. Shi YJ, Hu SJ, Zhao QQ, Liu XS, Liu C and Wang H: Toll-like receptor 4 (TLR4) deficiency aggravates dextran sulfate sodium (DSS)-induced intestinal injury by down-regulating IL6, CCL2 and CSF3. *Ann Transl Med* 7: 713, 2019.
48. Gross V, Andus T, Caesar I, Roth M and Schölmerich J: Evidence for continuous stimulation of interleukin-6 production in Crohn's disease. *Gastroenterology* 102: 514-519, 1992.
49. Han F, Li S, Yang Y and Bai Z: Interleukin-6 promotes ferroptosis in bronchial epithelial cells by inducing reactive oxygen species-dependent lipid peroxidation and disrupting iron homeostasis. *Bioengineered* 12: 5279-5288, 2021.
50. Li M, Jin S, Zhang Z, Ma H and Yang X: Interleukin-6 facilitates tumor progression by inducing ferroptosis resistance in head and neck squamous cell carcinoma. *Cancer Lett* 527: 28-40, 2022.
51. Kunzmann AT, Murray LJ, Cardwell CR, McShane CM, McMenamin UC and Cantwell MM: PTGS2 (Cyclooxygenase-2) expression and survival among colorectal cancer patients: A systematic review. *Cancer Epidemiol Biomarkers Prev* 22: 1490-1497, 2013.
52. Roberts PJ, Morgan K, Miller R, Hunter JO and Middleton SJ: Neuronal COX-2 expression in human myenteric plexus in active inflammatory bowel disease. *Gut* 48: 468-472, 2001.
53. Singer IL, Kawka DW, Schloemann S, Tessner T, Riehl T and Stenson WF: Cyclooxygenase 2 is induced in colonic epithelial cells in inflammatory bowel disease. *Gastroenterology* 115: 297-306, 1998.
54. Chiang SK, Chen SE and Chang LC: A dual role of heme oxygenase-1 in cancer cells. *Int J Mol Sci* 20: 39, 2018.
55. Chen Y, Wang J, Li J, Zhu J, Wang R, Xi Q, Wu H, Shi T and Chen W: Astragalus polysaccharide prevents ferroptosis in a murine model of experimental colitis and human Caco-2 cells via inhibiting NRF2/HO-1 pathway. *Eur J Pharmacol* 911: 174518, 2021.
56. Lipinski S, Till A, Sina C, Arlt A, Grasberger H, Schreiber S and Rosenstiel P: DUOX2-derived reactive oxygen species are effectors of NOD2-mediated antibacterial responses. *J Cell Sci* 122: 3522-3530, 2009.
57. Haberman Y, Tickle TL, Dexheimer PJ, Kim MO, Tang D, Karns R, Baldassano RN, Noe JD, Rosh J, Markowitz J, *et al*: Pediatric Crohn disease patients exhibit specific ileal transcriptome and microbiome signature. *J Clin Invest* 124: 3617-3633, 2014.
58. Gajendran M, Loganathan P, Catinella AP and Hashash JG: A comprehensive review and update on Crohn's disease. *Dis Mon* 64: 20-57, 2018.
59. Rolak S and Kane SV: Conventional therapies for Crohn's disease. *Gastroenterol Clin North Am* 51: 271-282, 2022.
60. Bian Y, Dong Y, Sun J, Sun M, Hou Q, Lai Y and Zhang B: Protective effect of kaempferol on LPS-induced inflammation and barrier dysfunction in a coculture model of intestinal epithelial cells and intestinal microvascular endothelial cells. *J Agric Food Chem* 68: 160-167, 2020.
61. Yuan Y, Zhai Y, Chen J, Xu X and Wang H: Kaempferol ameliorates oxygen-glucose deprivation/reoxygenation-induced neuronal ferroptosis by activating Nrf2/SLC7A11/GPX4 axis. *Biomolecules* 11: 923, 2021.



Copyright © 2024 Zhang et al. This work is licensed under a Creative Commons Attribution-NonCommercial-NoDerivatives 4.0 International (CC BY-NC-ND 4.0) License.